8-24-2004

Lithium Abundance and Isotope Systematics of Forearc Serpentinites, Conical Seamount, Mariana Forearc: Insights Into the Mechanics of Slab-Mantle Exchange During Subduction

Laurie D. Benton
arnegie Institution of Washington

Jeffrey G. Ryan
University of South Florida, ryan@usf.edu

Ivan P. Savov
University of South Florida, savovi@si.edu

Lithium abundance and isotope systematics of forearc serpentinites, Conical Seamount, Mariana forearc: Insights into the mechanics of slab-mantle exchange during subduction

Laurie D. Benton

Department of Terrestrial Magnetism, Carnegie Institution of Washington, 5241 Broad Branch Road, NW, Washington, D.C. 20015, USA

Exponent Environmental Group, 15375 30th Place, Suite 250, Bellevue, Washington 98007, USA (lbenton@exponent.com)

Jeffrey G. Ryan

Department of Terrestrial Magnetism, Carnegie Institution of Washington, 5241 Broad Branch Road, NW, Washington, D.C. 20015, USA

Department of Geology, University of South Florida, 4202 East Fowler Avenue, SCA 528, Tampa, Florida 33620–5201, USA (ryan@chuma.cas.usf.edu)

Temporarily at Division of Undergraduate Education, National Science Foundation, 4201 Wilson Boulevard, Arlington, Virginia 22230, USA

Ivan P. Savov

Department of Geology, University of South Florida, 4202 East Fowler Avenue, SCA 528, Tampa, Florida 33620–5201, USA (savovip@yahoo.com)

[1] Variable lithium contents and contrasting Li isotopic signatures are evident in the serpentininite muds and clasts extruded at Conical Seamount in the Mariana forearc. The muds have high Li contents compared to mantle values (3–7 ppm) and a mean δ^7Li value of ~+6‰. The clasts are generally lower in Li, and δ^7Li varies from −6‰ to +10‰, with higher δ^7Li correlating broadly to higher lithium contents. The diverse δ^7Li in the serpentinite clasts suggests Li exchanges between mantle rocks and evolving slab-derived fluids from different depths, producing a subarc mantle that is zoned in terms of Li abundances and δ^7Li. Mariana forearc Li isotopic signatures reach values as high as those reported in Mariana arc lavas, but neither Mariana lavas nor lavas from other "mature" arcs show the variability observed in the serpentinites. Although elevated serpentinite Li contents indicate forearc releases of Li, large differences in δ^7Li are not evident in the slab outputs at forearc versus arc depths in the Marianas, despite evidence for changes in other alkaline species (e.g., Ba, Sr, K). It is thus possible that the Li sampled by Mariana arc volcanoes is in large part Li which was released in the forearc and transported in the mantle via convection to arc depths, as has been proposed to explain B isotopic variations [*Straub and Layne*, 2002]. The uniform δ^7Li signatures observed in "mature" volcanic arcs [*Tomascak et al.*, 2002] are consistent with higher overall fluxes of slab fluids, which generate larger melting anomalies, including both modified and nonmodified mantle wedge domains. High or low δ^7Li in lavas from anomalous arcs (e.g., Panama [*Tomascak et al.*, 2000]) may indicate that the volumes of mantle sampled in these magmatic events are smaller and thus more likely to reflect the signatures of hydrated "plums" [e.g., *Allègre and Turcotte*, 1986; *Phipps Morgan and Morgan*, 1999] with extremely high or low δ^7Li.

1. Introduction

[2] The "slab input" to the mantle sources of arc lavas is a chemically complex flux within which a number of components have been identified: melts of subducted sediment [*Plank and Langmuir*, 1993; *Elliott et al.*, 1997], fluids from basaltic crust [*Miller et al.*, 1994; *Ishikawa and Nakamura*, 1994; *Class et al.*, 2000], melts of basaltic crust [*Kepezhinskas and Defant*, 1996] and fluids derived from subducted sediment [*Class et al.*, 2000]. While these different components can be recognized on discrimination diagrams, it is difficult to quantify their relative roles, as we have no physical or geochemical descriptions of them; i.e., if a fluid from sediment is involved, what is the overall makeup of this fluid phase (i.e., proportions of H_2O, CO_2, SO_2, halogens; pH; f_{O_2}) and what elements and/or chemical species does it transport at the depths of arc volcanic root zones? In the Mariana subduction system we have an opportunity to assess one particular slab outflux: an H_2O-dominated fluid release at low temperatures, which is absorbed into the mantle wedge via serpentinization reactions, and is thus measurable through analysis of the diapiric serpentinites erupting in the outer forearc region of the Mariana arc. This flux has been shown to mobilize a limited menu of "fluid mobile" species, which, interestingly, do not include elements such as Ba and U, that are normally used to fingerprint slab influences [*Pearce and Peate*, 1995; *Elliott et al.*, 1997; see also *Savov et al.*, 2000, 2002; *Morris and Ryan*, 2003].

[3] Lithium is an element that appears to be mobile in forearc settings, and it is unique among mobile elements in that it partitions well into olivine and other Mg silicates [*Ryan and Langmuir*, 1987; *Brenan et al.*, 1998a, 1998b; *Seitz and Woodland*, 2000]. Lithium abundance and isotope systematics may thus be able to provide a more detailed picture of how slab fluids interact with the mantle in forearc settings. Lithium isotopes show strong fractionations during solid-fluid exchanges due to the large mass difference between ^6Li and ^7Li [e.g., *Chan and Edmond*, 1988], and should thus allow us to assess how Li is moved from slab to mantle at arc or forearc depths. We report below on Li abundance and Li isotope data collected on serpentinite muds and serpentinized ultramafic rocks from the Conical Seamount, an active serpentinite mud volcano situated ~29 km above the downgoing slab in the Mariana forearc [*Fryer*, 1992].

2. Geologic Setting and Sample Selection

[4] The Conical Seamount lies at approximately 19°31′N Latitude, 146°40′W Longitude, at ~3000 m water depth, ~90 km inboard of the Mariana trench (Figure 1). All the forearc seamounts of the Mariana subduction system lie within zones of extensional faulting which run perpendicular to the strike of the trench. The seamount consists of sequences of serpentinite mudflows, and these flows include entrained clasts of highly serpentinized harzburgites and dunites [*Hussong and Fryer*, 1985; *Fryer et al.*, 1990; *Fryer*, 1992, 2002]. Mudflow activity is driven by the upwelling of an evolved, highly alkaline (pH 12.6), low-chlorinity (less than half that of seawater) pore fluid that originates from the dehydration of the subducting slab and is responsible for serpentinization reactions at depth. This fluid, sampled as pore waters in
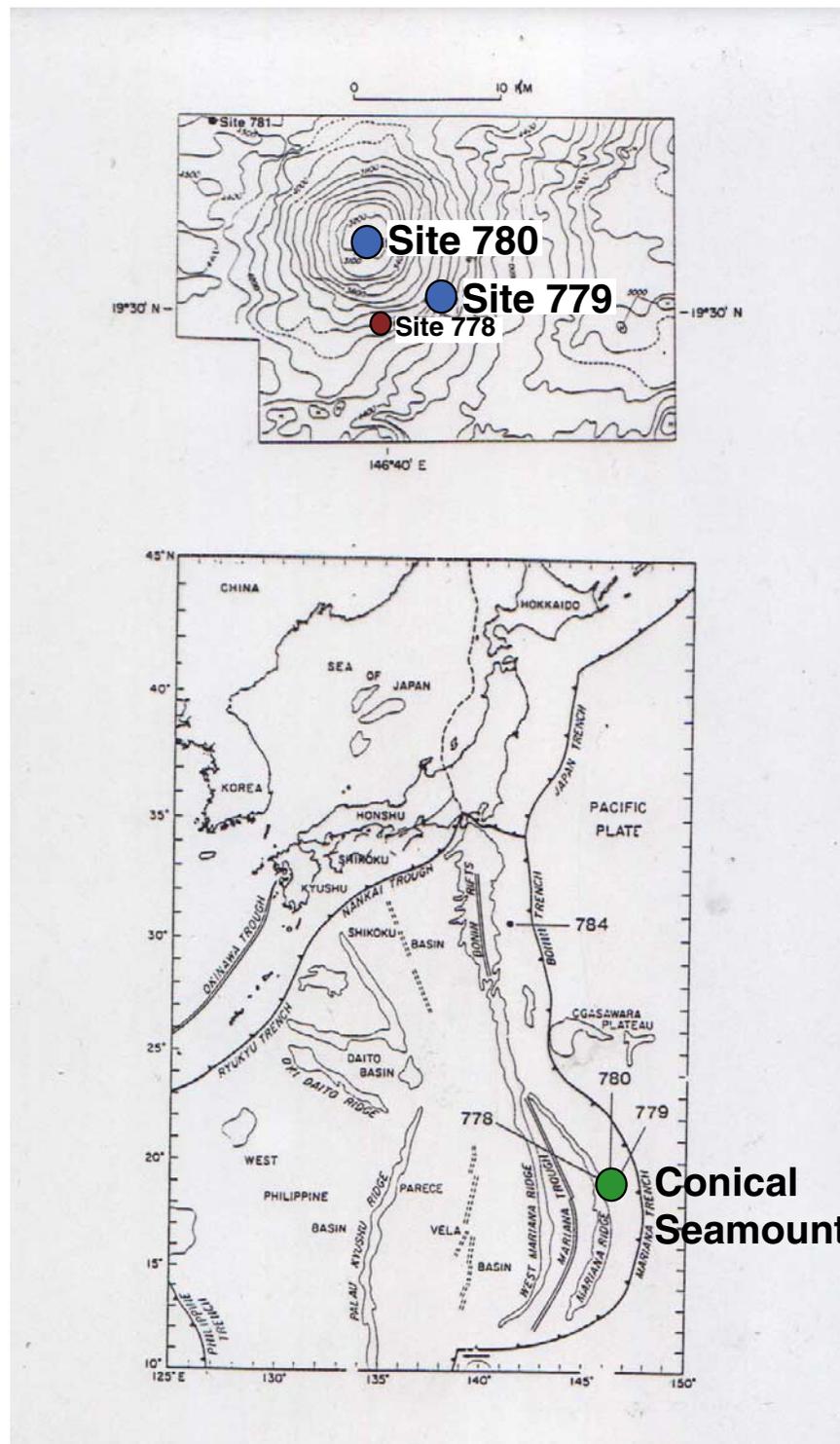
Figure 1. Map of the Mariana forearc region, with close-up of the Conical Seamount showing the location of Sites 779 and 780. From *Fryer* [1992].

the uppermost portion of the seamount (1–300 meters below seafloor (mbsf)), also has distinctive trace element signatures, including highly elevated B concentrations (~42 ppm, ~10x seawater) and Li contents (at ~11 ppb) that are more than three orders of magnitude lower than seawater [*Fryer et al.*, 1985; *Fryer and Fryer*, 1987; *Mottl*, 1992; *Mottl et al.*, 2003].

[5] During the Ocean Drilling Program (ODP) Leg 125, three sites on Conical Seamount were drilled: the summit (Site 780) and two flank sites (Sites 778 and 779; Figure 1 inset). Drill core from Holes 780C and 779A provide the longest sequences of serpentinite muds and clasts, and also include fragments of basaltic crustal rocks, as well as small pieces of blueschist-facies meta-mafic rocks which are probably derived from the downgoing plate [*Fryer and Fryer*, 1987; *Fryer*, 1992; *Maekawa et al.*, 1992, 1995]. Serpentinites (i.e., clasts and matrix collectively unless specified otherwise) from Site 780 are in intimate association with anomalous pore waters to within 3 m of the seafloor. Serpentinites from Site 779 are in contact with higher chlorinity pore waters, which show evidence for exchange with seawater, but preserve the high pH characteristics of the upwelling fluid at depths below ∼100 mbsf [*Fryer*, 1992; *Mottl*, 1992].

[6] Samples of the serpentinite muds were selected to examine the Li and Li isotope systematics of the evolving, slab-derived fluid, as data for B isotopes and other tracers suggest that the muds are in chemical equilibrium with the pore waters [*Benton et al.*, 2001; *Haggerty*, 1991; *Haggerty and Chaudhuri*, 1992; *Mottl*, 1992; *Mottl et al.*, 2003]. Samples of the entrained ultramafic clasts were examined in search of deeper-seated Li isotopic signatures, which might be more representative of conditions closer to the slab-mantle interface. Most of our samples are highly serpentinized (>60% serpentine) with loss on ignition (LOI) values between 8% and 24%. As pH, Sr isotope, and B isotope results indicate the influence of infiltrating seawater in shallow portions of Sites 779 and 780 (see above), we focused our sampling on deeper segments of cores, and followed the same protocols for sample selection and preparation as had been used for B isotopes (see below). As was the case with B and B isotopes, Li concentrations and Li isotope ratios appear unaffected by seawater in the deeper core segments at both sites. Shallower core sections show Li concentration and Li isotope variations similar to those found deeper, suggesting that overall, the influence of seawater may be negligible.

3. Methods

[7] We chose samples for analysis from both Site 779 (Holes A and B) and Site 780 (Holes C and D; Figure 1). Clast samples were selected from the interiors of relatively vein-free core segments, on the presumption that the interiors are less likely to suffer late-stage exchanges with seawater. However, it turned out to be impossible to avoid finer veins, so many of our samples included veined materials. Both the matrix and clast samples consisted of chrysotile ± lizardite or antigorite [*Mottl*, 1992; *Fryer*, 1992; *Heling and Schwarz*, 1992; *Lagabrielle et al.*, 1992; *Saboda et al.*, 1992]. Matrix samples were ground with an agate mortar and pestle and then washed with deionized water to remove salts from pore waters [*Spivack and Edmond*, 1987]. Clast samples were crushed, washed in deionized water, and powdered in a ball mill using an alumina vial dedicated to serpentinite samples.

[8] Samples analyzed for Li abundances were dissolved using an $HF:HClO_4$ digestion technique, and analyzed by standard additions methods via Direct Current Plasma emission spectrometry (DCP) (see *Ryan and Langmuir* [1987] for details on the method). A subset of the samples was analyzed for Li by isotope dilution mass spectrometry (IDMS) (see Table 1). Agreement between DCP and IDMS Li data is within the ±5% precision of the DCP analyses.

[9] Samples for Li isotope determinations were prepared via an $HF:HNO_3:HClO_4$ digestion, followed by a final dry-down in concentrated HNO_3, which was necessary to decompose abundant $Mg(ClO_4)_2$ generated in the breakdown of these Mg-rich rocks. Mg-perchlorates have a limited solubility in the 0.66 M HNO_3/33% methanol solutions loaded onto cation columns for Li elution, and could be observed as an immiscible liquid when present. Lithium isotope measurements on samples with Mg-perchlorate residues were anomalously high, suggesting some fractionation of the isotopes occurred when it was present. The addition of strong HNO_3 followed by a hard dry-down at ∼160°C resulted in clear solutions for all such samples, though in a few cases multiple dry-downs were necessary to decompose all of the Mg-perchlorates.

[10] For isotopic analysis, Li was isolated by ion-exchange chromatography using the methanol-HNO_3 method described by *Tomascak et al.* [1999a], and the final solutions were diluted to ∼100 ng Li/ml for analysis. Lithium isotope measurements were made on the VG P-54 multiple-collector magnetic sector ICP-MS at the Department of Terrestrial Magnetism according to procedures outlined by *Tomascak et al.* [1999b]. Each sample was measured a minimum of three times, and the measurements were averaged. Duplicates of several of our samples were prepared and analyzed as a further check on precision (see Table 1). On the basis of the total

Table 1. Lithium Abundance and Isotope Data for Conical Seamount Samples

Sample Identification[a]	Depth, mbsf	δ^7Li, ‰	Li, ppm
Serpentinite Matrix			
125-779A-			
05R-3, 054-056	32.75	+6.3	1.80
13R-1, 138-140	107.45		1.81
18R-2, 087-089	157.38	+7.2	0.76
28R-2, 112-114	227.60		1.47
32R-2, 000-010	265.95		1.04
36R-2, 132-134	305.85	+4.6	26.4
125-779B-			
01R-1, 117-119	1.18	+4.9	3.83
125-780C-			
02R-1, 002-004	5.53	+7.3	4.59
04R-1, 024-026	23.74	+6.2	4.66
05R-1, 037-039	33.37	+5.7	4.18
07R-1, 014-017	52.24	+4.3	2.89
12R-1, 006-008	100.26	+6.9	4.27
13R-1, 053-055	107.03	+5.2	2.23
15R-1, 027-029	125.77	+7.0	7.58
16R-1, 033-035	135.33	+6.8	5.83
18R-1, 129-131	155.29	+6.6	7.07
18R-1, 138-140	155.38	+7.3	6.55
duplicate		+7.5	
125-780D-			
01X-1, 026-028	0.26	+6.3	7.05
duplicate		+5.9	
02X-1, 035-037	2.85	+6.6	5.63
06X-2, 033-035	21.51	+7.1	7.52
07X-5, 123-125	29.31	+6.6	6.61
Serpentinized Peridotite Clasts			
125-779A-			
03R-CC, 015-016	10.76	+10.3	10.5
duplicate		+9.5	
06R-1, 020-022	39.22	+3.6	9.63
08R-1, 090-093	59.43	+2.8	3.31
11R-1, 016-018	87.48	−1.3	3.45
duplicate		−1.3	
13R-2, 053-054	108.64	+1.9	2.71
15R-2, 022-023	126.63	+2.0	8.43
17R-3, 123-125	149.45	+5.0	3.36
20R-1, 017-018	169.28	+10.2	12.9
duplicate		+8.1	
22R-2, 020-022	171.81	+6.4	4.35
25R-1, 029-030	197.10	+7.2	3.46
28R-3, 029-030	229.10	+7.3	2.79
31R-1, 057-058	255.28	+3.1	2.71
duplicate		+3.0	
33R-2, 082-083	276.33	+6.0	1.59
35R-1, 113-114	294.44	+4.0	5.65
125-780C			
03R-1, 3A	14.30	+3.5	18.9
06R-1, 7A	43.10	+1.1	3.21
08R-1, 5	61.95	+0.62	1.93
09R-1, 6	71.60	−6.1	1.63
10R-1, 2	80.90	+1.6	4.73
12R-1, 2	100.40	+5.7	16.2
13R-1, 7	106.90	+3.6	9.43
16R-1, 7	135.55	−0.8	4.18
18R-1, 055-057	154.55	−3.6	2.66
18R-1, 2B	155.20	-2.4	4.53

Table 1. (continued)

Sample Identification[a]	Depth, mbsf	δ^7Li, ‰	Li, ppm
Reference Materials			
UB-N serpentinite		−2.6	27[b]
JDF-D2 (MORB)		+6.8	7.8

[a] Sample identification is according to the following ODP convention: 125 (ODP Leg) - 779 (Site) A (Hole) - 05 (Core) R (drilling method, e.g., R for rotary and X for extended core barrel) - 3 (Section), 054–056 cm (Interval).

[b] Value from International Association of Geoanalysts Web site (http://www.geoanalyst.org).

errors of our sample measurements, and duplicate analyses of samples, our precision was at least as good as the ±1‰ (2σ) level reported for the ICP-MS method in the past [e.g., *Tomascak et al.*, 1999b, 2000].

4. Results

[11] Lithium abundance and Li isotope data for the Conical Seamount and relevant reference samples are presented in Table 1. Lithium concentrations in the serpentinized ultramafic clasts are quite variable, ranging from 0.9–18.9 ppm. The serpentinite matrix samples range from 1–8 ppm Li (with one outlier at 26.3 ppm), and are less variable in Li content (Figure 2). Lithium contents in Site 779 matrix samples appear to be lower than those from Site 780 (1–4 ppm versus 4–8 ppm, respectively; Figure 2). The very high Li concentration in sample 779A-36R-2, 132–134, the deepest sample analyzed (306 mbsf), probably cannot be generated purely via equilibrium exchange of serpentine with the associated, higher Li pore waters (0.2–0.8 ppm Li, higher than seawater [see *Mottl*, 1992]), especially given the low Li contents of other mud samples in contact with these fluids. The Li content in this sample may thus reflect the admixture of fine-grained mafic materials with higher Li and/or a higher affinity for Li during solid/fluid exchange [*Benton*, 1997; see also *Guggino et al.*, 2002; *Savov*, 2004].

[12] Lithium concentrations show no clear relationship to LOI in our samples, or to the abundances of other fluid-mobile, incompatible trace elements (Figure 3). The serpentinite matrix samples show a general positive variation relative to boron contents, but with several outliers at very high B or Li abundances. The cause for this diversity may be that, as noted above, mud samples may contain variable amounts of fine grained, altered mafic material (either blueschist-grade crustal material from the slab, or material from the overriding
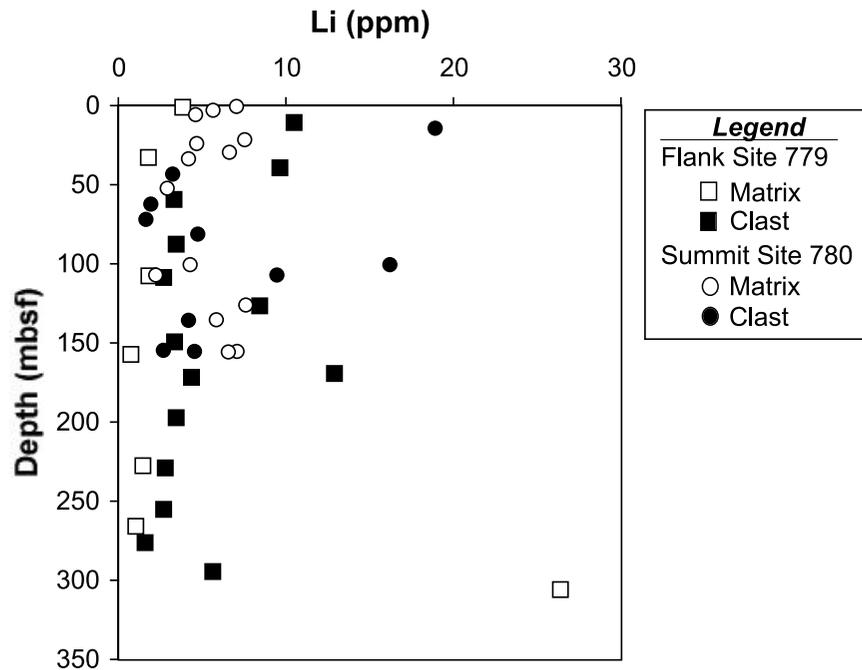
Figure 2. Plot of Li concentrations for Leg 125 serpentinites versus depth in core. Matrix and clast samples from each drill site are as noted on the diagram; matrix samples are open symbols, and clast samples are solid symbols.

crust), which could affect the systematics of these elements differently [*Benton*, 1997; *Guggino et al.*, 2002; *Savov*, 2004].

[13] Li isotopic variations in the clasts and muds contrast markedly. The serpentinite muds span a limited range of δ^7Li (+4 to +8‰), with a mean value near +6‰. The serpentinized clasts vary widely in δ^7Li, from −6‰ to +10‰ (Figure 4). This variation is not related to LOI or abundances of other mobile elements (Figure 5), but does show a broad relationship to Li content, with the higher Li clasts associated with generally higher δ^7Li values, and those samples with Li contents <5 ppm covering nearly the entire range of δ^7Li values observed (Figure 6).

5. Discussion

5.1. Origins of Li Distribution and δ^7Li Signatures in Conical Serpentinites

[14] Lithium concentrations in the Leg 125 serpentinites are generally elevated relative to their harzburgite or dunite protoliths [*Ryan and Langmuir*, 1987; *Seitz and Woodland*, 2000]. Interestingly, Li abundances are quite variable in the Leg 125 samples analyzed. The serpentinized clasts show the greatest degree of variation in this regard (up to 18.9 ppm Li) and also include a number of samples that approach the Li contents of depleted ultramafic
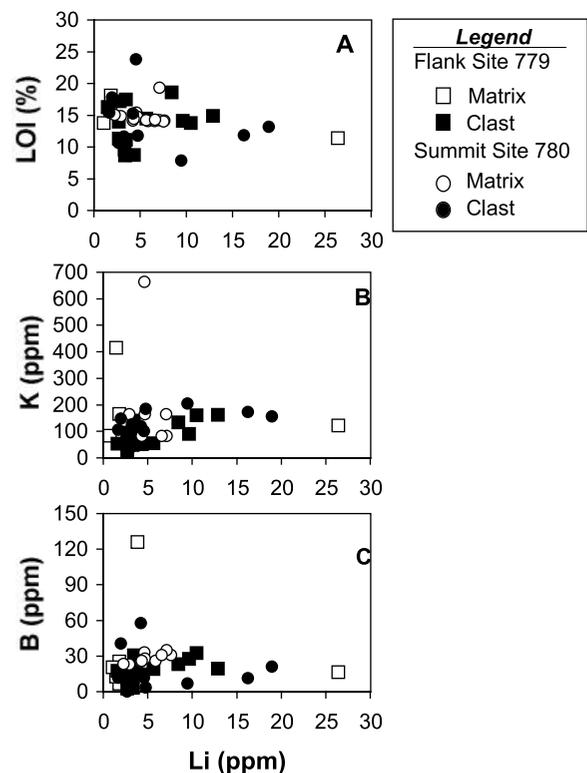
Figure 3. Plots of (a) Li concentrations versus LOI; (b) Li versus K concentrations; and (c) Li versus B concentrations for Leg 125 serpentinites. Additional data are from *Benton et al.* [2001] and *Mattie and Ryan* [1994].
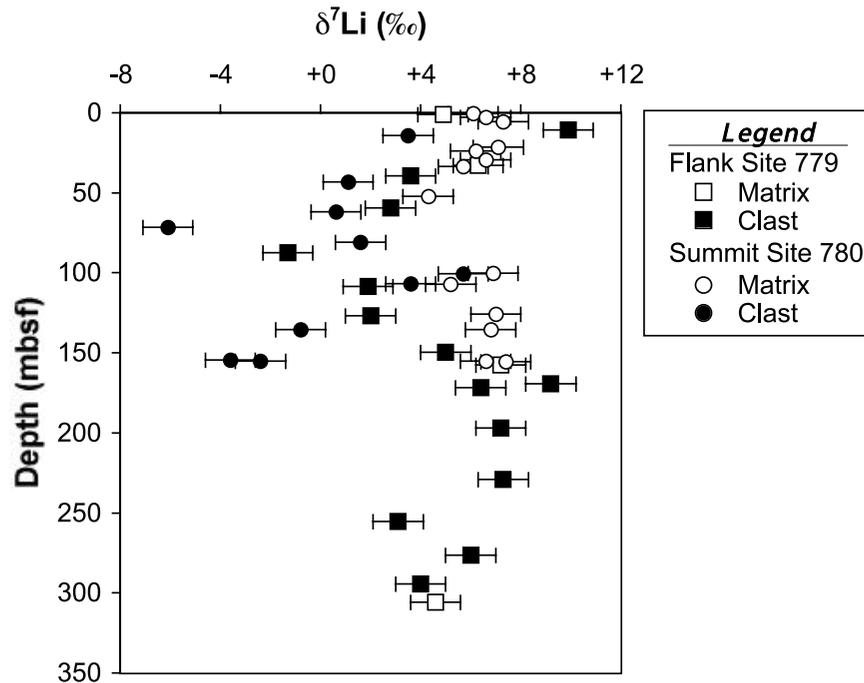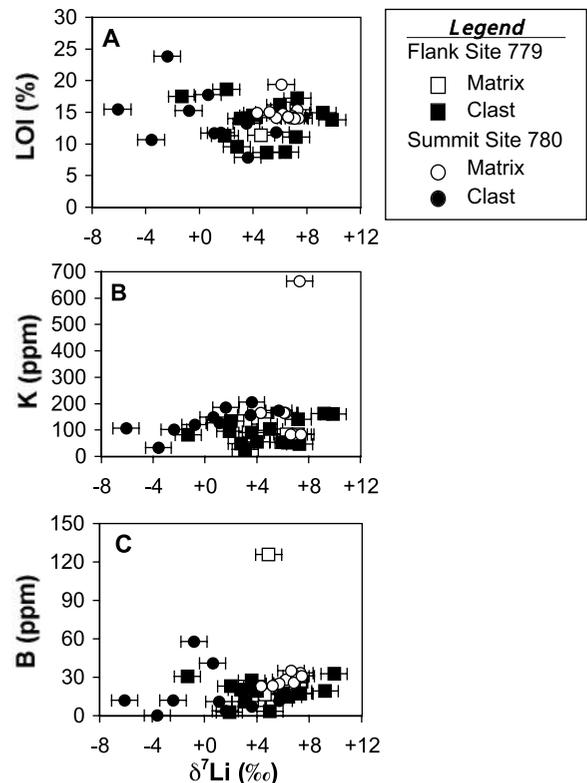
Figure 4. Plot of δ^7Li for Leg 125 serpentinites versus depth in core.

rocks (i.e., ~1−2 ppm [see *Ryan and Langmuir*, 1987; *Seitz and Woodland*, 2000]). Lithium contents in the serpentinite muds are, by contrast, generally more consistent. It is possible that Li contents in matrix serpentines reflect in some way the equilibration of these Mg-silicates with their associated pore waters: the upwelling, evolved slab-derived fluids at summit Site 780, and the seawater modified fluids found at flank Site 779.

[15] Lithium partitions strongly into serpentine under low-temperature conditions as seen with other sheet silicates [*Seyfried et al.*, 1984; *Scambelluri et al.*, 2004]. *Scambelluri et al.* [2004] suggest a $D_{Li}^{serpentine/fluid}$ of ~3.5 for dehydration reactions in Alpine serpentinites, and the mud/fluid ratio of Li concentrations between the Site 779 muds and pore waters are consistent with such a D value. The much higher mud/fluid ratio for Li at Site 780 requires progressive removal of Li from the upwelling fluids into serpentine, producing very Li-depleted pore waters near the surface.

[16] The large variation in Li contents and δ^7Li among the serpentinized clast samples argues against both simple models of equilibration with associated pore waters, or Rayleigh-style models for progressive removal. The ready uptake of Li by serpentine and other sheet silicates under low-temperature (<300°C) conditions [*Seyfried et al.*, 1984, 1998] means that Li from vein fluids will be

Figure 5. Plots of (a) δ^7Li versus LOI; (b) δ^7Li versus K concentrations; and (c) δ^7Li versus B concentrations for Leg 125 serpentinites. Additional data are from *Benton et al.* [2001] and *Mattie and Ryan* [1994].
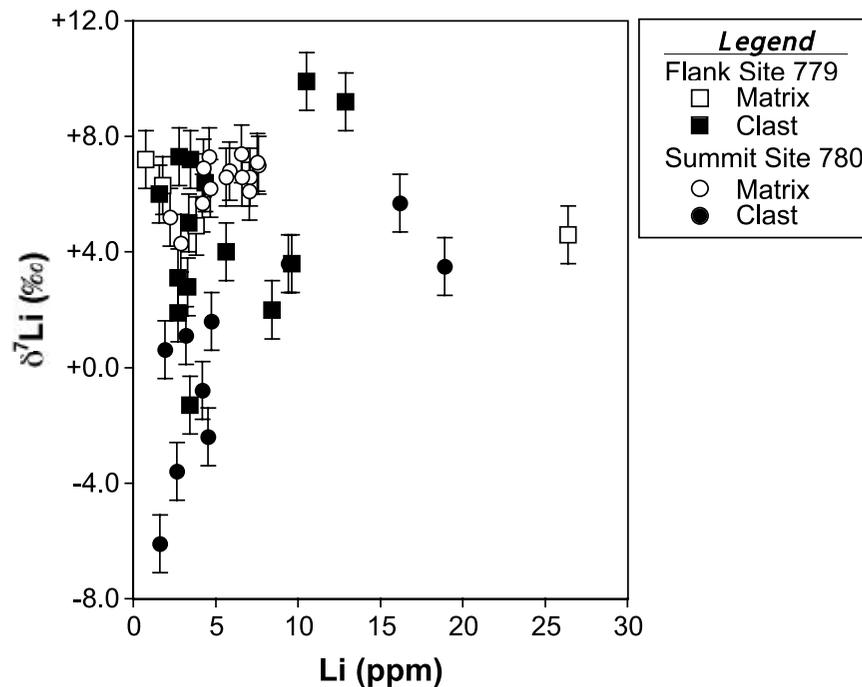
Figure 6. Plot of δ^7Li versus Li concentrations for Leg 125 serpentinites.

incorporated rapidly by forming serpentine, creating a Li "concentration front" near the vein that diminishes rapidly with distance from the vein (Figure 7). High Li in serpentinized clasts probably indicates proximity to veins providing Li-enriched slab fluids, while low-Li serpentinized clasts indicate modification by waters from which Li has been removed during earlier fluid-rock exchanges. The result of these sorts of progressive exchanges should be markedly variable Li contents in serpentinized mantle rocks [e.g., *Decitre et al.*, 2002].

[17] Lithium isotope systematics of the Conical serpentinites present a picture similar to that for Li abundances: the serpentinite matrix samples approach a mean δ^7Li value of +6‰, while the serpentinized clast samples show substantial variation, including values both lower and higher than the δ^7Li range of the matrix samples. Lithium isotope ratios in the Leg 125 serpentinite clast and matrix materials are similar to a first order to those found in oceanic serpentinites by *Decitre et al.* [2002]. However, data for the associated pore waters, and B isotope results on these same samples document that the role of seawater in the development of the Leg 125 serpentinites is negligible [*Benton et al.*, 2001; *Mottl*, 1992; *Mottl et al.*, 2003]. The similarity in Li isotope results for the Mariana forearc serpentinites and marine serpentinites documents that, as in the oceans, the Leg 125 samples have interacted with fluid phases that

had very high δ^7Li [*Chan and Edmond*, 1988; *Chan et al.*, 1992, 1994].

[18] Recently reported Li isotope data for pore waters from the South Chamorro serpentinite seamount (drilled during ODP Leg 195) point to exceptionally heavy signatures, with δ^7Li values greater than +40‰, suggesting fluid-serpentine fractionations of ~+30‰, assuming equilibrium exchange [see *Savov et al.*, 2002]. δ^7Li values like those of the serpentinite matrix samples reflect the mean Li isotopic signature imparted on the shallow mantle wedge by evolving slab fluids. This signature has a δ^7Li value lower than reported averages for the altered crustal and sedimentary constituents of downgoing slabs, which range from +8 to +14‰ [e.g., *Chan et al.*, 1992, 1994]. The δ^7Li signatures of our serpentinites are also considerably lower than the δ^7Li (up to +20‰) inferred for the forearc reservoir from recent studies of eclogites and high-grade metamorphic suites, which indicate that deeply subducted materials may have very low δ^7Li [*Zack et al.*, 2003]. Specific data for the Li isotope ratios of Mariana trench sediments and altered crust are not available, so it is not clear if the serpentinites preserve Li that is different isotopically from the probable slab "infeed" to the Mariana subduction system. However, these serpentinites are consistent with the kinds of Li isotopic signatures encountered in lavas from the Mariana arc system, and in other island arcs
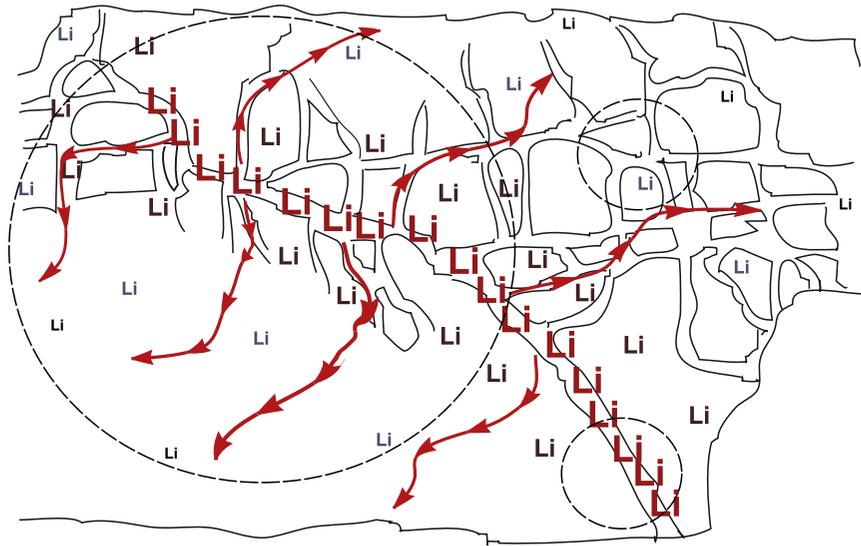
Figure 7. Sketch of a veined Mariana forearc serpentinite showing a likely pattern of Li distribution due to exchanges with vein fluids. Slab-derived fluids inject Li (red lettering), which is largely deposited in serpentine near the vein. Percolation of fluid outward from the vein forms serpentine with progressively lower Li content (brown to blue to black lettering). Subsequent fluid injections will overprint this pattern, producing serpentines with highly variable Li contents. Lithium isotope ratios in the forming serpentinite will vary on the basis of depths of fluid origin and the composition of the mantle, though high-Li samples will have higher δ^7Li (see also Figure 8). Dashed circles overlain on the sketch represent the kind of sampling of this modified mantle that could occur during melting: small F melts will preferentially sample the most hydrated portions of the subarc mantle, but these portions may have either high or low δ^7Li. Melting at larger values of F will average greater volumes of mantle, producing lavas with intermediate (and relatively uniform) δ^7Li.

[*Benton and Tera*, 2000; *Chan et al.*, 1999, 2001; *Elliott et al.*, 1997; *Moriguti and Nakamura*, 1998; *Tomascak et al.*, 2002].

5.2. Sources of Li Isotope Heterogeneity in the Forearc Mantle

[19] The Li isotopic diversity of the Leg 125 clasts is comparable to the in situ heterogeneity in Li isotopic compositions observed in seafloor serpentinites from the Southwest Indian Ridge [*Decitre et al.*, 2002]. Our serpentinite clast data shows a broad correlation to Li content (i.e., higher δ^7Li samples generally have higher Li abundances) and at the high end it overlaps the serpentinite mud data. However, there is a significant range in δ^7Li at both the high-Li and low-Li ends of the array (i.e., samples with >10 ppm Li have δ^7Li of +3.5 to +10‰, and samples with <2 ppm Li have δ^7Li of +6 to −6‰; Figure 6). The pattern in Figure 6 implies that higher δ^7Li clasts are produced via incorporation of slab-derived Li with a heavier Li isotopic composition, but the diversity in the data requires calling on a complex mixing process between the mantle wedge and slab-derived fluids of different compositions.

[20] Figure 8 describes one means for generating the δ^7Li variation in the clasts. Any fluid derived from the slab will carry Li with a δ^7Li value significantly higher than that of the slab, as all known solid/fluid fractionation processes for Li concentrate ^{7}Li in the hydrous fluid phase [*Chan and Edmond*, 1988; *Chan et al.*, 1992, 1994]. The degree of Li abundance enrichment in slab-derived fluids will depend on the temperature of fluid release, as $D_{Li}^{solid/fluid}$ is strongly temperature dependent between 100 and 400°C, with Li becoming more soluble where temperatures are higher [*Seyfried et al.*, 1984, 1998]. As well, the δ^7Li of slab fluids will become lower as the temperatures of fluid generation increase, because $\alpha_{Li}^{fluid/serpentine}$ declines with increasing temperature. Thus fluids released from the slab at relatively low temperatures (i.e., at shallow slab depths) will have lower Li contents, but higher δ^7Li, while fluids released at higher temperatures (i.e., greater depths) will have higher Li contents and lower δ^7Li. Progressive exchanges between such slab fluids and mantle rock in the shallow forearc will produce serpentinites with variable Li concentrations (due to the high $D_{Li}^{serpentine/fluid}$ [*Scambelluri et al.*, 2004]). Lithium isotope ratios in the forming
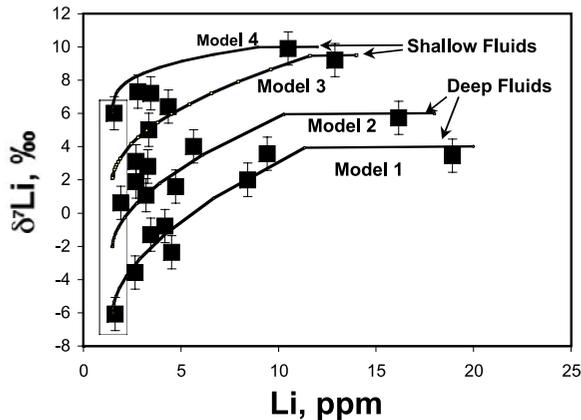
Figure 8. Plot of δ^7Li versus Li concentrations for the Leg 125 serpentinized clast samples. The four trend lines represent possible serpentine compositions developed during progressive fluid/rock serpentinization reactions with fluids derived from deeper (Models 1 and 2) and shallower (Models 3 and 4) portions of the slab. Serpentine compositions were calculated incrementally using the equilibrium fluid/rock exchange equation [*Nabelek*, 1987, equation (3)]: $C_r^f = (C_r^i + NC_w^i)/(D_s^l N + 1)$ for Li concentrations and $R_r^f = [((R_r^i + 1000) + N(R_w^i + 1000))/(\alpha_s^l N + 1)] - 1000$ for δ^7Li values. C_r represents concentrations in the rock, C_w is concentrations in the fluids, R_r is the δ^7Li of the rock, and R_w is the δ^7Li of the fluid; D_s^l is the fluid/solid distribution coefficient for Li (set at 3.5 [*Scambelluri et al.*, 2004]), and α_s^l is the Li isotope fractionation factor (set at 1.015, assuming higher temperatures than encountered during exchanges on the seafloor [e.g., *Chan et al.*, 1992]). Initial fluid Li concentrations and isotope ratios were estimated on the basis of the values necessary to produce the high-Li, high-δ^7Li samples along each trend. Fluid/rock ratios begin at 1.5 for the deep fluid trends and at 2.3 for the shallow fluid trends. The Li concentration of the mantle is set at 1.5 ppm [*Ryan and Langmuir*, 1987; *Seitz and Woodland*, 2000], while mantle δ^7Li values were selected to best approximate the trends of our data. Fluid/rock ratios were reduced with each increment calculated to reflect the incorporation of fluids into forming serpentines; increment sizes were kept small so as to approximate continuous fluid/rock exchange during serpentine formation. The large range of δ^7Li in both the high-Li and low-Li serpentinite clasts necessitates multiple fluid/rock exchange trajectories with fluids of different initial δ^7Li and lithium concentrations, and a mantle that is already zoned in terms of Li isotopic composition.

serpentinites will be related to the original δ^7Li values of the fluid and the mantle, and to the isotope fractionation factor for Li between serpentine and fluid (i.e., $\alpha_{Li}^{fluid/serpentine}$) at the temperature (i.e., depth) of exchange.

[21] The calculated fluid-rock exchange trajectories on Figure 8 reflect progressive serpentine formation due to the reaction of slab-derived fluids with the forearc mantle wedge. No single trajectory can explain the range of Li abundances and δ^7Li values observed in our Leg 125 clasts. However, a series of trajectories, reflecting exchanges with fluids possessing variable Li concentrations and δ^7Li, consistent with the signatures of fluids released from the slab at different depths, approximates the observed variation, assuming the mantle possesses significant variability in its Li isotopic signature before exchange (i.e., that mantle horizons already existed with δ^7Li from +6‰ to −6‰).

[22] *Nishio et al.* [2004] has reported δ^7Li signatures for mantle xenoliths ranging from +6 to −17‰, and attributes the lower values to exchanges with distinct metasomatizing agents derived from slab materials subducted to great depths. *Zack et al.* [2003] also infers the release of slab fluids at great depths to produce eclogites with δ^7Li of −11‰. A low-δ^7Li, deep-derived slab fluid percolating upward (i.e., down temperature) along the slab-mantle interface could react at shallower depths with upper mantle materials that have δ^7Li ≈ +3‰ to produce solids with lower δ^7Li, because the value of $\alpha_{Li}^{fluid/solid}$ at the depth of this reaction will be larger than at the depth from which the fluid originated. Exchanges between deep-derived slab fluids and upper mantle materials in the forearc may be a viable mechanism for creating zones of variable δ^7Li in the mantle.

5.3. Implications for Li Isotope Systematics in Volcanic Arcs

[23] Significant heterogeneity in radiogenic isotopic signatures (i.e., $^{87}Sr/^{86}Sr$, $^{143}Nd/^{144}Nd$, U-Th-Pb) is well documented in mantle rocks [*Nishio et al.*, 2004; *Reisberg and Zindler*, 1986; *Reisberg et al.*, 1989; and references therein]. Variations in radiogenic isotope ratios within an ultramafic massif can be as great or greater than the total isotopic variation observed in mantle-derived volcanic rocks [see *Reisberg et al.*, 1989, Figure 10]. The range of δ^7Li values in our Leg 125 clasts is larger than the total Li isotopic variation among all igneous rocks thus far examined. The highest values in our suite (at +9.9‰) are only slightly lower than the highest δ^7Li ever reported in an arc, +11.2‰ in the Panama arc segment of Central America [*Tomascak et al.*, 2000]. So, as with radiogenic isotope systems, Li isotope ratios may record fine-scale geochemical variations in mantle

source materials. This variation arises from multi-stage additions of exotic (in this case, slab-derived) components, and isotopic exchange under multiple P-T conditions.

[24] Modeling the Li isotope systematics of subduction zones as a simple mixture of slab-derived and mantle-derived Li, as is often done in examining isotopic variations in arcs, is problematic because of the complex manner in which slab lithium is added to the subarc mantle, and the significant redistribution of Li that occurs as a result of such additions. *Straub and Layne* [2002] explained unusually high $\delta^{11}B$ values in tephra glasses from the Izu arc through mechanical inputs to subarc source regions of forearc derived, high $\delta^{11}B$ serpentinized mantle materials via drag convection [e.g., *Tatsumi*, 1986]. Our Li isotope results for Conical serpentinites indicate that such a model is a permissible explanation of observed Li isotope systematics in the Mariana arc, and in other "mature" subduction systems where the observed Li isotopic variation is limited [e.g., *Benton and Tera*, 2000; *Chan et al.*, 1999, 2001; *Tomascak et al.*, 2002]. However, arcs in which Li isotopic compositions both heavier and lighter than those in the Mariana arc system are encountered (e.g., Panama [*Tomascak et al.*, 2000]) cannot be easily explained in this manner.

[25] Perhaps the best model for understanding the Li isotopic diversity that results from slab inputs, and relating this diversity to the Li isotopic signatures of arcs, is to call upon the "plum pudding" type models used to explain mantle reservoir mixing and magmatic sampling at ocean islands and seamounts [*Allègre and Turcotte*, 1986; *Batiza and Vanko*, 1984; *Phipps Morgan and Morgan*, 1999]. Vein serpentine and highly hydrated ultramafic materials near veins will have high Li and variably high $\delta^{7}Li$, while the variably serpentinized mantle between zones of veining will have lower Li concentrations, and $\delta^{7}Li$ values ranging from those of typical upper mantle (i.e., MORB-like) to exceptionally low values, perhaps reflecting exchanges with deep slab fluids (Figure 7). If these complexly modified mantle materials convect to depth and became part of a subarc mantle source, both the hydrated higher $\delta^{7}Li$ materials, and the hydrated low-$\delta^{7}Li$ mantle rocks will be more liable to melt. Thus, at low values of melt fraction (F), either high-$\delta^{7}Li$ or low-$\delta^{7}Li$ melts (or melts consisting of mixtures of these end-member materials, dominated by the higher Li abundance end-member) might occur, as initial melts will be dominated

by hydrated mantle components. As F increases, more of the mantle source melts, and proportionally less hydrated mantle material will be sampled by melting, which should shift the mean $\delta^{7}Li$ of the forming magmas away from extreme values, and closer to an average value for upper mantle rocks. In "mature" arcs such as the Mariana subduction system, the Kuril arc and others, values for F are generally high, so $\delta^{7}Li$ approaches MORB-like values [*Benton and Tera*, 2000; *Tomascak et al.*, 2002]. In anomalous arc settings, such as Panama, [e.g., *Defant et al.*, 1991; *Tomascak et al.*, 2000] magmatism is more sporadic, F is necessarily lower, and Li isotope ratios may thus approach some of the more extreme values encountered in the Mariana forearc mantle.

5.4. Comparisons to B Isotope Systematics in Arcs and Implications for Li Isotopes as a "Tool" in Studies of Subduction Zones

[26] Given the differences in their solid-fluid behaviors in forearc settings, the B and Li isotopic systems provide distinctly different types of information about the slab-mantle exchange processes occurring during subduction. Boron abundances and B isotopes provide a fingerprint of the slab fluid input, while Li abundances and Li isotopes provide insights into how this fluid input modifies and hybridizes the subarc mantle. The "decoupling" of Li isotopes and B/Be systematics in Panama arc lavas reported by *Tomascak et al.* [2000] is consistent with the behavioral characteristics of these elements: boron tracks slab fluid inputs exclusively, while Li "sees" subduction-generated mantle heterogeneity beneath the Panamanian arc, and not just the signature of the most recent fluid inputs (Figure 9). Mantle heterogeneity beneath volcanic arcs is evident only where the "slab effect" is minimized [see *Edwards et al.*, 1993; *Lin et al.*, 1990]. In the case of Li, preserved mantle heterogeneity may be related to past slab-mantle exchange events, so presumably Li isotopic variations in arc lavas will only be identifiable in the case of "dying" arcs, where subduction rates and associated slab fluid inputs have diminished.

6. Conclusions

[27] Serpentinite muds from the Mariana forearc have Li isotope ratios lower overall than many probable slab materials, but similar to Mariana arc lavas. The associated serpentinized ultramafic clasts preserve heterogeneous $\delta^{7}Li$ signatures, reflecting a complex history of exchanges between
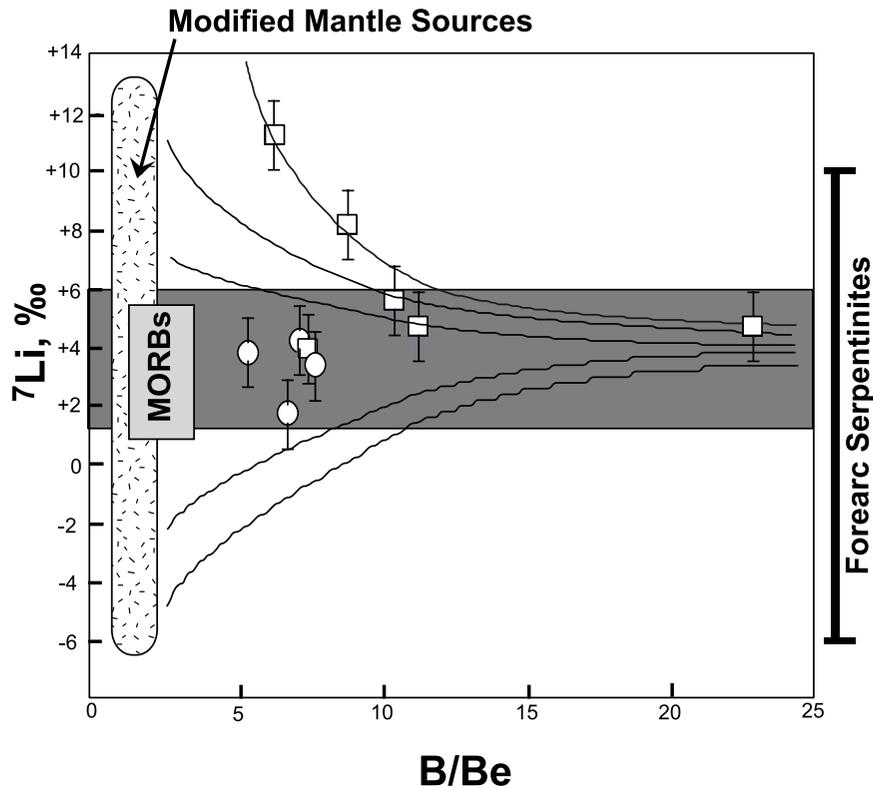
Figure 9. Plot of δ^7Li versus B/Be for arc lavas. The darkly shaded field across the diagram represents the combined δ^7Li arc data sets of *Chan et al.* [1999, 2001] and *Tomascak et al.* [2002], which constitute most of the available data on "normal" arcs, and overlaps entirely with the range for MORBs (labeled [*Tomascak and Langmuir*, 1999]). The symbols represent Old Group (squares) and Young Group (circles) arc lavas from Panama [*Tomascak et al.*, 2000]. The range of δ^7Li for the Mariana forearc serpentinites is shown by the large bracket to the right of the plot. The stippled vertical field represents the range of possible δ^7Li signatures developed in the mantle wedge over time via slab fluid exchange, and the curves represent hypothetical mixing arrays between these mantle reservoirs and slab fluid, which has high B/Be, and (in most arcs) relatively MORB-like δ^7Li.

Li-bearing, slab-derived fluids and the forearc mantle wedge. Melting beneath arcs mixes Li-enriched mantle horizons with unaltered mantle rocks, producing δ^7Li values only modestly different from those of MORBs. Only in anomalous circumstances can the Li isotope heterogeneity of the mantle be observed in the compositions of arc lavas.

Acknowledgments

References

Allègre, C. J., and D. L. Turcotte (1986), Implications of a two-component marble-cake mantle, *Nature*, *323*, 123–127.

Batiza, R., and D. Vanko (1984), Petrology of young Pacific seamounts, *J. Geophys. Res.*, *89*, 1235–1260.

Benton, L. D. (1997), Origin and evolution of serpentine seamount fluids, Mariana and Izu-Bonin forearcs: Implications for the recycling of subducted material, Ph.D. dissertation, Univ. of Tulsa, Tulsa, Okla.

Benton, L. D., and F. Tera (2000), Lithium isotope systematics of the Marianas revisited, *Goldschmidt J. Conf. Abstr.*, *5*, 210.

Benton, L. D., J. G. Ryan, and F. Tera (2001), Boron isotope systematics of slab fluids as inferred from a serpentinite

seamount, Mariana forearc, *Earth Planet. Sci. Lett.*, *187*, 273–282.

Brenan, J. M., E. Neroda, C. C. Lindstrom, H. F. Shaw, F. J. Ryerson, and D. L. Phinney (1998a), Behaviour of boron, beryllium and lithium during melting and crystallization: Constraints from mineral-melt partitioning experiments, *Geochim. Cosmochim. Acta*, *62*, 2129–2141.

Brenan, J. M., F. J. Ryerson, and H. F. Shaw (1998b), The role of aqueous fluids in the slab-to-mantle transfer of boron, beryllium, and lithium during subduction: Experiments and models, *Geochim. Cosmochim. Acta*, *62*, 3337–3347.

Chan, L.-H., and J. M. Edmond (1988), Variation of lithium isotope composition in the marine environment: A preliminary report, *Geochim. Cosmochim. Acta*, *52*, 1711–1717.

Chan, L.-H., J. M. Edmond, G. Thompson, and K. Gillis (1992), Lithium isotopic composition of submarine basalts: Implications for the lithium cycle in the oceans, *Earth Planet. Sci. Lett.*, *108*, 151–160.

Chan, L.-H., J. M. Gieskes, C.-F. You, and J. M. Edmond (1994), Lithium isotope geochemistry of sediments and hydrothermal fluids of the Guaymas Basin, Gulf of California, *Geochim. Cosmochim. Acta*, *58*, 4443–4454.

Chan, L.-H., W. P. Leeman, and C.-F. You (1999), Lithium isotopic composition of Central American volcanic arc lavas: Implications for modification of the sub-arc mantle by slab-derived fluids, *Chem. Geol.*, *160*, 255–280.

Chan, L.-H., W. P. Leeman, and C.-F. You (2001), Lithium isotopic composition of Central American volcanic arc lavas: Implications for modification of the sub-arc mantle by slab-derived fluids: Correction, *Chem. Geol.*, *182*, 293–300.

Class, C., D. M. Miller, S. L. Goldstein, and C. H. Langmuir (2000), Distinguishing melt and fluid subduction components in Umnak Volcanics, Aleutian Arc, *Geochem. Geophys. Geosyst.*, *1*, Paper number 1999GC000010.

Decitre, S., E. Deloule, L. Reisberg, R. James, P. Agrinier, and C. Mével (2002), Behavior of Li and its isotopes during serpentinization of oceanic peridotites, *Geochem. Geophys. Geosyst.*, *3*(1), 1007, doi:10.1029/2001GC000178.

Defant, M. J., L. F. Clark, R. H. Stewart, M. S. Drummond, J. Z. de Boer, R. C. Maury, H. Bellon, T. E. Jackson, and J. F. Restrepo (1991), Andesite and dacite genesis via contrasting processes: The geology and geochemistry of El Valle Volcano, Panama, *Contrib. Mineral. Petrol.*, *106*, 309–324.

Edwards, C. M. H., J. D. Morris, and M. F. Thirlwall (1993), Separating mantle from slab signatures in arc lavas using B/Be and radiogenic isotope systematics, *Nature*, *362*, 530–533.

Elliott, T., T. Plank, A. Zindler, W. White, and B. Bourdon (1997), Element transport from subducted slab to juvenile crust at the Mariana arc, *J. Geophys. Res.*, *102*, 14,991–15,019.

Fryer, P. (1992), A synthesis of Leg 125 drilling of serpentine seamounts on the Mariana and Izu-Bonin forearcs, *Proc. Ocean Drill. Program Sci. Results*, *125*, 593–614.

Fryer, P. (2002), Recent studies of serpentinite occurrences in the oceans: Mantle-ocean interactions in the plate tectonic cycle, *Chem. Erde*, *62*, 257–302.

Fryer, P., and G. J. Fryer (1987), Origins of nonvolcanic seamounts in a forearc environment, in *Seamounts, Islands, and Atolls*, *Geophys. Monogr. Ser.*, vol. 43, edited by B. H. Keating et al., pp. 61–69, Washington, D. C.

Fryer, P., E. L. Ambos, and D. M. Hussong (1985), Origin and emplacement of Mariana forearc seamounts, *Geology*, *13*, 774–777.

Fryer, P., K. L. Saboda, L. B. Johnson, M. E. Mackay, G. F. Moore, and P. Stoffers (1990), Conical Seamount: Sea-

MARK II, *Alvin* submersible, and seismic reflection studies, *Proc. Ocean Drill. Program Initial Rep.*, *125*, 69–80.

Guggino, S., I. P. Savov, and J. G. Ryan (2002), Light element systematics of metamorphic clasts from ODP Legs 125 and 195, South Chamorro and Conical Seamounts, Mariana forearc, *Eos Trans. AGU*, *83*(19), Spring Meet. Suppl., Abstract V51A-08.

Haggerty, J. A. (1991), Evidence from fluid seeps atop serpentine seamounts in the Mariana forearc: Clues for emplacement of the seamounts and their relationship to forearc tectonics, *Mar. Geol.*, *102*, 293–309.

Haggerty, J. A., and S. Chaudhuri (1992), Strontium isotopic composition of the interstitial waters from Leg 125: Mariana and Bonin forearcs, *Proc. Ocean Drill. Program Sci. Results*, *125*, 397–400.

Heling, D., and A. Schwarz (1992), Iowaite in serpentinite muds at Sites 778, 779, 780 and 784: A possible cause for the low chlorinity of pore waters, *Proc. Ocean Drill. Program Sci. Results*, *125*, 313–323.

Hussong, D. M., and P. Fryer (1985), Fore-arc tectonics in the Northern Mariana Arc, in *Formation of Active Ocean Margins*, edited by N. Nasu et al., pp. 273–290, Terra Sci., Tokyo.

Ishikawa, T., and E. Nakamura (1994), Origin of the slab component in arc lavas from across-arc variation of B and Pb isotopes, *Nature*, *370*, 205–208.

Kepezhinskas, P., and M. J. Defant (1996), Contrasting styles of mantle metasomatism above subduction zones: Constraints from ultramafic xenoliths, in Kamchatka, in *Subduction: Top to Bottom*, *Geophys. Monogr. Ser.*, vol. 96, edited by G. E. Bebout et al., pp. 307–314, AGU, Washington, D. C.

Lagabrielle, Y., A.-M. Karpoff, and J. Cotton (1992), Mineralogical and geochemical analyses of sedimentary serpentinites from Conical Seamount (Hole 778A): Implications for the evolution of serpentine seamounts, *Proc. Ocean Drill. Program Sci. Results*, *125*, 325–342.

Lin, P. N., R. J. Stern, J. D. Morris, and S. H. Bloomer (1990), Nd- and Sr-isotopic compositions of lavas from the northern Mariana and southern Volcano arcs: Implications for the origin of island arc melts, *Contrib. Mineral. Petrol.*, *105*, 381–392.

Maekawa, H., M. Shozui, T. Ishii, K. L. Saboda, and Y. Ogawa (1992), Metamorphic rocks from the serpentine seamounts in the Mariana and Izu-Ogasawara forearcs, *Proc. Ocean Drill. Program Sci. Results*, *125*, 415–430.

Maekawa, H., P. Fryer, and A. Ozaki (1995), Incipient blueschist-facies metamorphism in the active subduction zone beneath the Mariana forearc, in *Active Margins and Marginal Basins of the Western Pacific*, *Geophys. Monogr. Ser.*, vol. 88, edited by B. Taylor and J. Natland, pp. 281–289, AGU, Washington, D. C.

Mattie, P. D., and J. G. Ryan (1994), Boron and alkaline element systematics in serpentinites from Holes 779A, 780C, and 784A, ODP Leg 125 describing fluid-mediated slab additions, *Eos Trans. AGU*, *75*, Fall Meet. Suppl., F352.

Miller, D. M., C. H. Langmuir, and S. L. Goldstein (1994), Cerium/lead and lead isotope ratios in arc magmas and the enrichment of lead in the continents, *Nature*, *368*, 514–520.

Moriguti, T., and E. Nakamura (1998), Across-arc variation of Li isotopes in lavas and implications for crust/mantle recycling at subduction zones, *Earth Planet. Sci. Lett.*, *163*, 167–174.

Morris, J. D., and J. G. Ryan (2003), Subduction zone processes and implications for changing composition of the upper and lower mantle, in *Treatise on Geochemistry*, edited

by R. Carlson, chap. 2, pp. 451–470, Elsevier Sci., New York.

Mottl, M. J. (1992), Pore waters from serpentine seamounts in the Mariana and Izu-Bonin Forearcs, Leg 125: Evidence for volatiles from the subducting slab, *Proc. Ocean Drill. Program Sci. Results*, *125*, 373–385.

Mottl, M. J., S. C. Komor, P. Fryer, and C. L. Moyer (2003), Deep-slab fluids fuel extremophilic *Archaea* on a Mariana forearc serpentinite mud volcano: Ocean Drilling Program Leg 195, *Geochem. Geophys. Geosyst.*, *4*(11), 9009, doi:10.1029/2003GC000588.

Nabelek, P. I. (1987), General equations for modeling fluid/rock interaction using trace elements and isotopes, *Geochim. Cosmochim. Acta*, *51*, 1765–1769.

Nishio, Y., S. Nakai, J. Yamamoto, H. Sumino, T. Matsumoto, V. S. Prikhod'ko, and S. Arai (2004), Lithium isotopic systematics of the mantle-derived ultramafic xenoliths: Implications for EM1 origin, *Earth Planet. Sci. Lett.*, *217*, 245–261.

Pearce, J. A., and D. W. Peate (1995), Tectonic implications of the composition of volcanic arc magmas, *Annu. Rev. Earth Planet. Sci.*, *23*, 251–285.

Phipps Morgan, J., and W. J. Morgan (1999), Two-stage melting and the geochemical evolution of the mantle: A recipe for mantle plum-pudding, *Earth Planet. Sci. Lett.*, *170*, 215–239.

Plank, T., and C. H. Langmuir (1993), Tracing trace element from sediment input to volcanic output at subduction zones, *Nature*, *362*, 739–742.

Reisberg, L., and A. Zindler (1986), Extreme isotopic variations in the upper mantle: Evidence from Ronda, *Earth Planet. Sci. Lett.*, *81*, 29–45.

Reisberg, L., A. Zindler, and E. Jagoutz (1989), Further Sr and Nd isotopic results from peridotites of the Ronda ultramafic complex, *Earth Planet. Sci. Lett.*, *96*, 161–180.

Ryan, J. G., and C. H. Langmuir (1987), The systematics of lithium abundances in young volcanic rocks, *Geochim. Cosmochim. Acta*, *51*, 1727–1741.

Saboda, K. L., P. Fryer, and H. Maekawa (1992), Metamorphism of ultramafic clasts from Conical Seamount: Sites 778, 779, and 780, *Proc. Ocean Drill. Program Sci. Results*, *125*, 431–443.

Savov, I. P. (2004), Petrology and geochemistry of subduction-related rocks from the Mariana arc-basin system, Ph.D. dissertation, 355 pp., Univ. of South Fla., Tampa.

Savov, I. P., J. G. Ryan, P. Mattie, and J. Schijf (2000), Fluid-mobile element systematics of ultramafic xenoliths from the Izu-Bonin-Mariana forearc: Implications for the chemical cycling in subduction zones, *Eos Trans. AGU*, *81*(48), Fall Meet. Suppl., Abstract V21C-02.

Savov, I. P., J. G. Ryan, L. Chan, M. D'Antonio, M. Mottl, P. Fryer, and ODP Leg 195 Sci. Party (2002), Geochem-istry of serpentinites from the S. Chamorro Seamount, ODP Leg 195, Site 1200, Mariana Forearc—Implications for recycling at subduction zones, *Goldschmidt J. Conf. Abstr.*, *7*, A670.

Scambelluri, M., O. Müntener, L. Ottolini, T. T. Pettke, and R.Vannucci (2002), The fate of B, Cl, and Li in the subducted oceanic mantle and in the antigorite breakdown fluids, *Earth Planet. Sci. Lett.*, *204*, 217–234.

Seitz, H. M., and A. B. Woodland (2000), The distribution of lithium in peridotitic and pyroxenitic mantle lithologies: An indicator of magmatic and metasomatic processes, *Chem. Geol.*, *166*, 47–64.

Seyfried, W. E., Jr., D. R. Janecky, and M. J. Mottl (1984), Alteration of the oceanic crust: Implications for the geochemical cycles of lithium and boron, *Geochim. Cosmochim. Acta*, *48*, 557–569.

Seyfried, W. E., Jr., X. Chen, and L.-H. Chan (1998), Trace element mobility and lithium isotope exchange during hydrothermal alteration of seafloor weathered basalt: An experimental study at 350°C, 500 bars, *Geochim. Cosmochim. Acta*, *62*, 949–960.

Spivack, A. J., and J. M. Edmond (1987), Boron isotope exchange between seawater and the oceanic crust, *Geochim. Cosmochim. Acta*, *51*, 1033–1043.

Straub, S. M., and G. D. Layne (2002), The systematics of boron isotopes in Izu arc front volcanic rocks, *Earth Planet. Sci. Lett.*, *198*, 25–39.

Tatsumi, Y. (1986), Formation of the volcanic front in subduction zones, *Geophys. Res. Lett.*, *13*, 717–720.

Tomascak, P. B., and C. H. Langmuir (1999), Lithium isotope variability in MORB, *Eos Trans. AGU*, *80*(46), Fall Meet. Suppl., F1086–F1087.

Tomascak, P. B., R. W. Carlson, and S. B. Shirey (1999a), Accurate and precise determination of Li isotopic compositions by multi-collector sector ICP-MS, *Chem. Geol.*, *158*, 145–154.

Tomascak, P. B., F. Tera, R. T. Helz, and R. J. Walker (1999b), The absence of lithium isotope fractionation during basalt differentiation: New measurements by multi-collector sector ICP-MS, *Geochim. Cosmochim. Acta*, *63*, 907–910.

Tomascak, P. B., J. G. Ryan, and M. J. Defant (2000), Lithium isotope evidence for light element decoupling in the Panama sub-arc mantle, *Geology*, *28*, 507–510.

Tomascak, P. B., E. Widom, L. D. Benton, S. L. Goldstein, and J. G. Ryan (2002), The control of lithium budgets in island arcs, *Earth Planet. Sci. Lett.*, *196*, 227–238.

Zack, T., P. B. Tomascak, R. L. Rudnick, C. Dalpe, and W. F. McDonough (2003), Extremely light Li in orogenic eclogites: The role of isotope fractionation during dehydration in subducted oceanic crust, *Earth Planet. Sci. Lett.*, *208*, 279–290.